The topography contribution to the influence of the atmospheric boundary layer at high altitude stations

Martine Collaud Coen[1], Elisabeth Andrews[2,3], Diego Aliaga[4], Marcos Andrade[4], Hristo Angelov[5], Nicolas Bukowiecki[6], Marina Ealo[7], Paulo Fialho[8], Harald Flentje[9], A. Gannet Hallar[10,11], Rakesh Hooda[12,13], Ivo Kalapov[5], Radovan Krejci[14], Neng-Huei Lin[15], Angela Marinoni[16], Jing Ming[17,18], Nhat Anh Nguyen[19], Marco Pandolfi[7], Véronique Pont[20], Ludwig Ries[21], Sergio Rodríguez[22], Gerhard Schauer[23], Karine Sellegri[24], Sangeeta Sharma[25], Junying Sun[26], Peter Tunved[14], Patricio Velasquez[27] and D. Ruffieux[1]

Supplement:

Calculation of the diurnal and seasonal cycles:

To obtain a statistically estimation of the diurnal cycles of a time series x(t), the following steps were applied for each month of the year:

1) We calculate the auto-correlation function (ACF) and the partial auto-correlation function (PACF) with the Levinson-Durbin recursion function of matlab (see Fig. S1 a and b).
2) The first lag auto-correlation a(k=1) corresponding to the auto-correlation at 1 hour since we have hourly temporal resolution is removed leading to a whitened new time series y(t):

$$y(t+1) = x(t+1) - a(k=1) * x(t)$$

3) We calculate the ACF and PACF of the whitened time series y(t) and the error corresponding to the upper and lower confidence limits for the auto-correlation (see Fig. S1 c). Only the auto-correlation that are statistically significant, that is higher than the error, are taken into account.
4) The maxima and minima of aerosol parameters do not follow a clear diurnal pattern due to several meteorological factors such as the occurrence of precipitation or of cloud and to various synoptic factors such as the advection of air masses of various origins. The auto-correlation will therefore not be always found at exactly 24 hours, so that the diurnal cycles were taken as the sum of the 22 to 26 lags (red square on Fig.S1 d).

The same analysis is performed on the whole dataset to determine the seasonal cycle, and the sum of PACF at lags 350 to 380 of the whitened time series is taken as amplitude of the seasonal cycle. The strength of the auto-correlation calculated by the PACF depends on both the regularity of the cycle and on its amplitude. Since the noise is very high for aerosol parameters, we can assimilate the strength of the PACF to the amplitude of the temporal cycles.

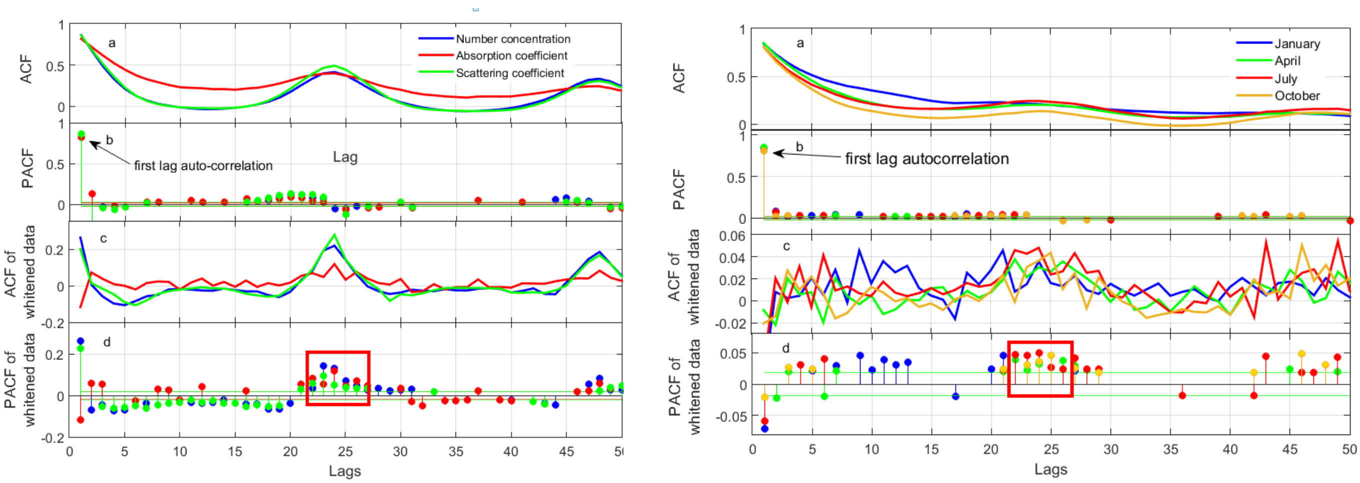

Figures S1: Auto-correlation function, partial auto-correlation function of the time serie x(t) (a and b) and of the whitened function y(t) (c and d) for the MLO aerosol number concentration, the absorption and scattering coefficients for January on the left figure and for the JFJ number concentration and 4 months of the year on the right figure.

Table S1: Instruments type, size cut and length of the used datasets in this paper. It has to be mentioned that some stations do have longer datasets that were for various reasons not used in their whole extent.

Station	Absorption coef. Scattering coef. Number concentration	Used time period	Size cut
BEO	CLAP TSI 3563 --	2012-2016 2007-2016 --	TSP
CHC	MAAP Ecotech, 3000 TSI 3772	2012-2015 2012-2015 2012-2015	TSP
CMN	MAAP Ecotech TSI 3772	2008-2015 2007-2015 2008-2015	TSP
HPB	MAAP TSI 3563 TSI 3772	2009-2012 2006-2015 2006-2015	PM10

IZO	MAAP	2007-2016	TSP
	TSI 3563	2008-2016	
	TSI 3025A	2008-2010	
JFJ	AE31	2001-2015	TSP
	TSI 3563	2001-2015	
	TSI 3772	2001-2015	
LLN	PSAP+CLAP	2008-2015	PM10
	TSI 3563	2008-2015	
	TSI 3010	2008-2015	
MLO	PSAP+CLAP	2001-2014	PM2.5 until July 2014
	TSI 3563	2001-2014	PM10 after July 2014
	TSI 3760	2001-2014	
MSA	MAAP	2011-2016	PM10
	Ecotech	2011-2016	
	--	--	
MSY	MAAP	2011-2015	PM10
	Ecotech 3000	2010-2015	
	--	--	
MUK	AE31	2005-2013	PM2.5
	Ecotech M 9003	2005-2013	
	DMPS	2005-2013	
NCOS	AE31	2010-2014	TSP
	--	--	
	--	--	
NWR	--	--	TSP
	MRI	1993-1996	
	TSI 3760	1993-1996	
OMP	AE31	2001-2005	TSP
	--	--	
	--	--	
PUY	MAAP	2008-2014	TSP
	TSI 3563	2006-2014	
	TSI 3010	2005-2014	
PDI	AE31	2014-2016	TSP
	Ecotech Aurora 3000	2014-2016	
	--		
PDM	AE16	2013-2016	TSP
	--	--	
	TSI 3010	2012-2016	
PEV	PSAP	2007-2009	TSP
	--	--	
	TSI 3010	2007-2009	
PYR	MAAP	2008-2013	MAAP @ TSP
	--	2006-2008	TSI 3563 @ PM10
	--	--	

SBO	AE33 Ecotech 4000 TSI 3022A	2013-2015 2013-2015 2013-2015	TSP
SPL	PSAP+CLAP TSI 3563 TSI 3010	2011-2016 2011-2016 2012-2016	PM10
SUM	PSAP+CLAP TSI 3563 --	2011-2015 2011-2015 --	PM2.5
TLL	AE31 Ecotech Aurora 3000 --	2013-2016 2013-2016 --	TSP until 1.12.2016 PM10 after 1.12.2016
WHI	PSAP+CLAP TSI 5363 TSI 3775	2008-2010 2008-2010 2008-2013	TSP for TSI 3775 PM2.5 until July 2009, PM1 thereafter
WLG	PSAP TSI 3563 TSI 3010	2005-2015 2005-2015 2006-2015	PM10/ PM1 PM10/ PM1 TSP
ZEP	AE31 TSI 3010, 3563 --	2005-2015 2010-2014 --	AE31 @ PM10 TSI 3010 @ TSP
ZSF	MAAP TSI 3563 TSI 3772	2009-2015 2010-2015 2009-2014	PM0.8 until 2012 and PM20 after 2012
ZUG	-- TSI 3563 --	-- 2010-2012 --	

Table S2: Kendall's tau correlation coefficients between the aerosol parameters percentiles and diurnal and seasonal cycles and the topographical parameters. The s.s. at 95% and 90% confidence levels are given in magenta and cyan, respectively.

Kendall's tau correlation coef.		ABL-TopoIndex	Altitude	Latitude	G8	LocSlope	Hypso %	HyspD50	DBinv
Absorption coef.	5%	**0.46**	-0.20	-0.20	-0.18	**-0.44**	**0.51**	**-0.33**	0.11
	50%	**0.34**	-0.12	**-0.35**	**-0.31**	**-0.34**	**0.44**	-0.14	0.15
	95%	**0.27**	-0.070	-0.26	**-0.30**	-0.19	**0.34**	-0.01	0.19
Scattering coef.	5%	**0.30**	-0.10	**-0.50**	-0.19	-0.22	**0.47**	-0.24	-0.17
	50%	0.26	-0.23	**-0.47**	-0.22	-0.21	**0.40**	-0.19	-0.05
	95%	0.050	-0.21	**-0.33**	-0.14	0.04	0.23	-0.04	-0.16

Number concentration	5%	**0.36**	-0.10	-0.12	**-0.38**	**-0.36**	**0.47**	-0.30	-0.16
	50%	**0.54**	-0.19	0.10	**-0.34**	**-0.49**	**0.56**	**-0.47**	-0.03
	95%	**0.41**	-0.32	-0.080	**-0.43**	**-0.41**	**0.43**	**-0.47**	-0.21
Absorption coef.	Dmin	**0.36**	-0.17	**-0.31**	-0.22	**-0.29**	**0.40**	-0.11	0.25
	Dmax	**0.32**	-0.040	**-0.42**	**-0.32**	-0.20	**0.37**	-0.05	0.17
	Season	0.15	0.11	-0.15	-0.08	-0.26	0.01	-0.23	-0.05
Scattering coef.	Dmin	0.11	-0.15	-0.27	0.12	-0.16	0.20	0.09	-0.03
	Dmax	0.12	0.010	**-0.52**	-0.05	-0.10	**0.31**	0.10	-0.09
	Season	0.030	**0.36**	-0.15	-0.25	-0.08	-0.02	-0.12	-0.18
Number concentration	Dmin	0.08	0.03	**-0.69**	**-0.49**	-0.26	0.08	0.05	-0.18
	Dmax	0.15	-0.15	**-0.56**	**-0.46**	-0.28	0.10	-0.08	-0.10
	Season	-0.28	-0.18	-0.18	-0.03	0.21	-0.28	0.15	0.08

Table S3: Liste of hyps% for all stations.

Station	Hyps%	Station	Hyps%	Station	Hyps%	Station	Hyps%	Station	Hyps%
APP	1.29	IZO	0.10	MTA	5.58	PUY	5.58	WHI	2.33
ASK	0.00	JFJ	0.03	MUK	37.99	PYR	20.66	WLG	36.15
BEO	0.00	LAN	48.99	MWO	0.00	RUN	1.81	YEL	10.45
CHC	0.14	LLN	0.53	MZW	5.85	SBO	0.08	ZEP	39.53
CMN	7.02	LQO	42.75	NAM	58.23	SHN	0.72	ZSF	1.31
FWS	0.00	MBO	0.03	NWR	2.28	SPL	1.69	ZUG	0.45
HAC	0.01	MKN	0.12	OMP	0.05	SUM	0.00		
HLE	55.62	MLO	1.93	PEV	0.01	SZZ	43.89		
HPB	19.92	MSA	3.43	PDI	19.78	TDE	0.00		
HPO	1.74	MSY	34.54	PDM	0.01	TLL	41.40		

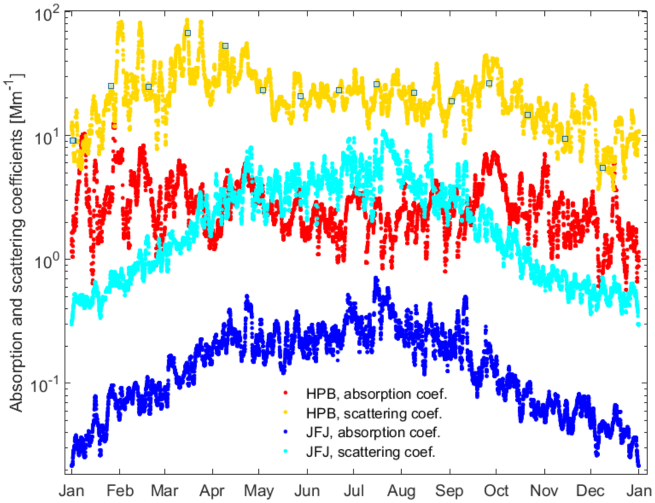

Figure S2: Seasonal cycles of the absorption and scattering coefficients of HPB and JFJ.